ORIGINAL ARTICLE

Ultrasmall Superparamagnetic Iron Oxide Nanoparticles as Emerging Contrast Agents for Enhanced T2-Weighted Magnetic Resonance Imaging

Mahboobeh Mehrabifard [1], Solmaz Derakhshan [2], Roqaie Kalantari [3], Amirhossein Rashnoodi [4], Saadat Ebrahimiyan [5], Sahar Mohammadjani [3], Omid Talaee [6*], Navid Kheradmand [7*]

[1] *Department of Radiology, Faculty of Paramedicine, Hormozgan University of Medical Sciences, Bandar Abbas, Iran*

[2] *Department of Internal Medicine, Kosar Hospital, Kurdistan University of Medical Sciences, Sanandaj, Iran*

[3] *Department of Medical Physics, School of Medicine, Iran University of Medical Sciences, Tehran, Iran*

[4] *Department of Medical Physics and Biomedical Engineering, Faculty of Medicine, Shahid Beheshti University of Medical Sciences, Tehran, Iran*

[5] *Department of Medical Physics and Radiology, School of Medicine, Gonabad University of Medical Sciences, Gonabad, Iran*

[6] *Department of Nuclear Engineering, Faculty of Mechanical Engineering, Shiraz University, Shiraz, Iran*

[7] *Department of Health Physics, Graduate School of Health Sciences, İstanbul Medipol University, İstanbul, Türkiye*

*Corresponding Authors: Omid Talaee, Navid Kheradmand
Emails: omid.talaee77@gmail.com, kheradmandnavid2@gmail.com

Received: 03 August 2024 / Accepted: 19 September 2024

Abstract

Purpose: Integrating magnetic Nanoparticles (NPs) into contrast-enhanced Magnetic Resonance (MR) imaging can significantly improve the resolution and sensitivity of the resulting images, leading to enhanced accuracy and reliability in diagnostic information. The present study aimed to investigate the use of targeted trastuzumab-labeled iron oxide (TZ-PEG-Fe_3O_4) NPs to enhance imaging capabilities for the detection and characterization of Breast Cancer (BC) cells.

Materials and Methods: The NPs were synthesized by loading Fe_3O_4NPs with the monoclonal antibody TZ. Initially, Fe_3O_4 NPs were produced and subsequently coated with Polyethylene Glycol (PEG) to form PEG- Fe_3O_4 NPs. The TZ antibody was then conjugated to the PEG- Fe_3O_4 NPs, resulting in TZ-PEG-Fe_3O_4 NPs. The resulting NPs were characterized using standard analytical techniques, including UV-Vis spectroscopy, FTIR, SEM, TEM, VSM, and assessments of colloidal stability.

Results: Analyses indicated that the targeted TZ-PEG-Fe_3O_4 NPs exhibited a spherical morphology and a relatively uniform size distribution, with an average diameter of approximately 60 nm. These results confirmed the successful synthesis and controlled fabrication of the Fe_3O_4 NPs, which is crucial for developing effective Contrast Agents (CAs) for medical imaging applications. Additionally, the study confirmed the biocompatibility and magnetic properties of the synthesized TZ-PEG-Fe_3O_4 NPs.

Conclusion: The findings suggest that the developed targeted TZ-PEG-Fe_3O_4 NPs have significant potential as effective CAs for MR imaging of BC cells.

Keywords: Fe_3O_4 Nanoparticles; PEGylating; Molecular Imaging; Magnetic Resonance Imaging; Breast Cancer.

Copyright © 2026 Tehran University of Medical Sciences.
This work is licensed under a Creative Commons Attribution-NonCommercial 4.0 International license (https://creativecommons.org/licenses/by-nc/4.0/). Noncommercial uses of the work are permitted, provided the original work is properly cited.
DOI: https://doi.org/10.18502/fbt.v13i3.22741

1. Introduction

Magnetic Resonance Imaging (MRI) has modernized the field of medical diagnostics by providing high-resolution, non-invasive visualization of anatomical structures and physiological processes within the body [1]. However, the inherent contrast in MRI images is often insufficient to clearly delineate tissues of interest. To address this limitation, Contrast Agents (CAs) have been advanced to heighten the image contrast and improve diagnostic accuracy [2, 3].

One class of CAs that has gained significant attention in recent years is Ultra-Small Superparamagnetic Iron oxide (USPIO) Nanoparticles (NPs) [4]. These NPs, with less than 20 nm diameter, possess unique magnetic features that make them highly effective as MRI CAs. When exposed to a strong magnetic field, the magnetic moments of the iron oxide (Fe_3O_4) NPs align, creating a local magnetic field distortion that affects the relaxation of nearby protons. This interaction leads to a curbing of the transverse relaxation time (T2), resulting in a decline in signal intensity on T2-weighted MR images [5]. The application of metal oxide NPs as MRI CAs has several advantages. These NPs can provide faster and more accurate detection of pathological changes in various tissues, especially in the early stages of diseases [6]. Additionally, the versatility of these NPs allows for their functionalization with targeting moieties, enabling the selective accumulation of the CAs in specific tissues or disease sites, further enhancing the diagnostic capabilities of MRI [7]. Furthermore, the development of multifunctional NPs that combine the contrast enhancement properties of metal oxides with therapeutic capabilities, such as drug delivery or magnetic hyperthermia [8], has opened up new avenues for the integration of diagnosis and treatment, known as theranostics. This method has the talent to considerably advance patient outcomes by providing a personalized and targeted approach to disease management [9].

The small size of USPIO NPs offers several advantages over larger superparamagnetic Fe_3O_4 NPs. First, their small diameter allows for efficient extravasation from blood vessels and enhanced tumor penetration, particularly when combined with external magnetic fields. This aspect is crucial for targeting and imaging solid tumors, where the Enhanced Permeability and Retention (EPR) effect can be exploited to selectively accumulate the NPs within the tumor tissue [8]. Second, the ultra-small size of SPIO NPs enables them to be unfurnished from the body through renal filtration, reducing the risk of long-term accumulation and potential toxicity. This is in contrast to larger SPIO particles, which are primarily taken up by the Reticuloendothelial System (RES) and cleared more slowly [10]. Third, USPIO NPs can be readily functionalized with various targeting ligands, such as antibodies (such as Trastuzumab (TZ)), peptides, or small molecules, to enhance their specificity towards disease-associated biomarkers. This allows for the progress of targeted CAs that can detect and monitor specific pathological processes, such as inflammation, angiogenesis, or apoptosis. One such targeting moiety is the monoclonal antibody TZ, which binds specifically to the human epidermal growth factor receptor 2 (HER-2) protein [11]. HER-2 is overexpressed in roughly 20% of BC cases, and its overexpression is related to a more destructive form of the disease. By conjugating TZ to the USPIO NPs, the resulting contrast agent can selectively target and accumulate in HER-2 positive BC cells, enabling enhanced visualization and potential theranostic applications [12]. Suitable surfactants such as dextran and Polyethylene Glycol (PEG) are usually used as coating materials to stabilize the suspension and prevent particles from settling, as well as loading antibodies or other drugs. For example, magnetite NPs coated with polyacrylic acid have been shown to exhibit good suspension stability at pH values below 5 [13]. Additionally, core-shell structured NPs with a Fe_3O_4 core and SiO2 shell have been synthesized with the silica layer acting as a suitable stabilizing coating. Furthermore, iron oxide NPs coated with PEG have also been investigated as MRI CAs, as the PEG stabilizer helps maintain proper nanoparticle suspension and stability [14, 15]. The careful design and selection of nanoparticle size and surface coatings are crucial factors in developing effective and stable MRI CAs. In-vivo studies have also demonstrated the potential of USPIO NPs as CAs for numerous applications, including cancer treatment – imaging [16], inflammation detection, and lymph node mapping [17]. These studies have highlighted the importance of optimizing the nanoparticle formulation, surface properties, and administration route to maximize their targeting efficiency and minimize potential side effects.

Despite the promising results, there are still challenges and limitations associated with the use of USPIO NPs as MRI CAs. One key challenge is the need for further optimization of the nanoparticle properties to enhance their targeting specificity and minimize non-specific

uptake by the RES. So, the USPIO NPs have emerged as promising CAs for enhanced T2-weighted MRI. Their small size, versatile surface properties, and unique magnetic characteristics make them attractive candidates for various diagnostic applications. As research in this field continues to advance, it is expected that USPIO NPs play an increasingly significant role in the early detection, monitoring, and management of various diseases, ultimately leading to improved patient outcomes. This research aims to develop targeted MRI CAs by synthesizing TZ-conjugated iron oxide (TZ-PEG-Fe_3O_4) NPs. These targeted NPs are designed to selectively accumulate in HER-2 positive BC cells, enabling enhanced visualization and potential theranostic applications.

2. Materials and Methods

2.1. Materials

The following chemicals were purchased: ferric chloride hexahydrate ($FeCl_3 \cdot 6H_2O$), ferric chloride tetrahydrate ($FeCl_2 \cdot 4H_2O$), 25% ammonia solution, bovine serum albumin (BSA, ≥96% purity), and DMSO from Merck Chemicals GmbH, Germany. Additionally, PEG-SH (molecular weight 2 kDa) was obtained from IrisHB Biotech in Germany. The cell lines used in this research, SKBr-3 (BC cells) and MCF-10A (non-cancerous cells), were acquired from the National Iranian Cell Bank.

2.2. Production of Nano-Compound

2.2.1. Synthesis of Fe_3O_4 NPs

The Fe_3O_4 NPs were synthesized using a method adapted from the protocol described by Cai *et al.* [22]. Briefly, 8 mL of a 2 M $FeCl_2$ solution and 2 mL of a 4 M $FeCl_2$ solution were combined and stirred for 40 minutes. This combined solution was then added to 100 mL of a 1.4 M ammonia solution. During this time, the Fe_3O_4 NPs precipitated out of the solution. The precipitate was then obtained through magnetic separation. Next, the precipitate was mixed with 50 mL of diluted 2 M perchloric acid ($HClO_4$) to create a colloidal suspension. Lastly, the final colloidal was separated by centrifugation, and the remaining solution was diluted with water to a total volume of 100 mL. This allowed us to isolate the synthesized Fe_3O_4 NPs for further characterization and use in subsequent experiments [18].

2.2.2. Preparation of TZ-Conjugated PEGylated Fe_3O_4 NPs

In this investigation, a novel class of multi-functional NPs for potential use in cancer imaging and targeted therapy TZ-labeled PEGylated iron oxide (TZ-PEG-Fe_3O_4) NPs was developed. The synthesis process involved several key steps. First, the Fe_3O_4 NPs were coated with PEG-SH to create PEGylated Fe_3O_4 NPs. This PEG coating helped to stabilize the NPs and improve their biocompatibility. Next, the PEGylated Fe_3O_4 NPs were further functionalized by covalently linking the monoclonal antibody TZ to the PEG linker. This was achieved by adding the TZ-PEG-OPSS in a PBS solution with a pH of 7.5. The OPSS end of the PEG linker was able to form a covalent bond with the NPs surface, effectively attaching the TZ to the Fe_3O_4 NPs. The PEGylation of the Fe_3O_4 NPs was carried out using a specific protocol. 100 mL of the thiolated PEG was added to 1 mL of the Fe_3O_4 NPs (1 mg/mL), followed by the immediate addition of 30 mL of the as-prepared PEGylated TZ. This entire process was conducted at a temperature of 4°C within 1 hour. The magnetic Fe_3O_4 NPs were then stabilized by the shorter chain of PEG-SH and collected using an external magnetic device [19].

2.3. Characterization of Advanced NPs

The morphology and size of the synthesized NPs thoroughly were characterized using advanced microscopy techniques such as Transmission Electron Microscopy (TEM) using a JEM-1400 microscope (Jeol, Peabody, MA, USA). Additionally, Scanning Electron Microscopy (SEM) was employed to further analyze the NPs structure. To investigate the chemical composition and successful synthesis of the NPs, the researchers utilized several complementary analytical techniques. Fourier-Transform Infrared (FTIR) spectroscopy was recorded using a Shimadzu Prestige-21 spectrometer (Shimadzu Corp., Kyoto, Japan). The FTIR spectra were assessed in the range of 4000 cm-1 to 400 cm^{-1}, which allowed for the identification of specific functional groups and confirmed the accurate synthesis of the PEGylated

NPs. Furthermore, the successful synthesis of the TZ-PEGylated Fe_3O_4 NPs was verified using UV-visible (UV-Vis) spectroscopy. The UV-Vis analysis provided additional evidence for the effective functionalization of the NPs with the TZ antibody. Moreover, the magnetic properties of the functionalized NPs were calculated using a Vibrating Sample Magnetometer (VSM). The tests were accompanied at room temperature under a maximum applied magnetic field of 8 kOe, using a VSM instrument provided by Meghnatis Daghigh Kavir Kashan Co. (Iran). This technique allowed for the assessment of the magnetic behavior and characteristics of the advanced NPs, which is an important consideration for their potential use in biomedical applications, such as MRI [1].

2.4. Colloidal Stability Test

Moreover, in order to assess the colloidal stability of TZ-PEG-Fe_3O_4 NPs, their hydrodynamic size was monitored using Dynamic Light Scattering (DLS) analysis over a period of seven days in a simulated biological environment of PBS at pH 7.4. The purpose of this investigation was to ensure that the NPs would remain stable and suitable for biological applications [8].

2.5. MTT Assay Test

To assess the cytotoxic effects of the synthesized samples, we utilized the widely used MTT assay. This colorimetric technique evaluates cell metabolic activity and viability, providing insights into the potential cytotoxicity of the advanced NPs. Cells were seeded into 96-well plates at a density of 105 cells per well and incubated for 24 hours to allow for cell attachment and growth. After the initial incubation period, varying concentrations of the NP samples, including TZ, Fe_3O_4 NPs, and TZ-PEG-Fe_3O_4 NPs, were added to the respective wells. The cells were then further incubated for 24 hours to enable the assessment of dose-dependent cytotoxic effects. During the 24-hour treatment, the viable, metabolically active cells converted the MTT reagent into purple-colored formazan products. An ELISA plate reader was used to measure the Optical Density (OD) of each well, which is directly proportional to the number of viable cells. The absorbance readings were taken at a wavelength of 570 nm, a commonly used wavelength for evaluating the metabolic activity and viability of cells. To ensure the reliability and accuracy of the results, the MTT assay and cell viability measurements were repeated three times, with the cells being exposed to varying concentrations of the different NP formulations in each replicate [19].

2.6. Relaxivity Measurements

To evaluate the MRI properties of the Fe_3O_4 and TZ-PEG-Fe_3O_4 NPs, we acquired T2-weighted phantom images. The NP samples were dispersed in water at different iron (Fe) concentrations, which were acquired using Inductively Coupled Plasma (ICP) analysis. The T2-weighted MR images were obtained using a Multi-Spin Echo (MSE) pulse sequence with the following imaging parameters: Repetition Time (TR) = 2,500 ms, Echo Times (TE) = 13, 28, 39, 52, 66, 79, 92, 105, and 118 millisecond (ms), slice thickness = 2 mm, Field Of View (FOV) = 250 mm × 250 mm, and matrix size = 384 × 512. These tests were achieved on a 1.5 T human clinical MRI scanner equipped with a head coil, with the samples maintained at room temperature [16].

2.7. Statistical Analysis

The results were presented as the mean ± Standard Deviation (SD), which provides a measure of the variability and uncertainty associated with the data. To determine the statistical significance of the findings, we performed one-way Analysis of Variance (ANOVA) and paired t-tests. The ANOVA allowed us to assess the overall differences among the experimental groups, while the paired t-tests enabled the comparison of specific pairs of data points.

3. Results

3.1. Nano-Complex Characterization Tests

The synthesis of Fe_3O_4 NPs was successfully achieved under specific conditions following established protocols as shown in Figure 1. To enhance the functionality of the synthesized NPs for biomedical applications, a cross-linker was employed to covalently attach PEG chains to the surface of the TZ, resulting in the covalent attachment of PEGylated TZ to the surface of the Fe_3O_4 NPs (Figure 1a).

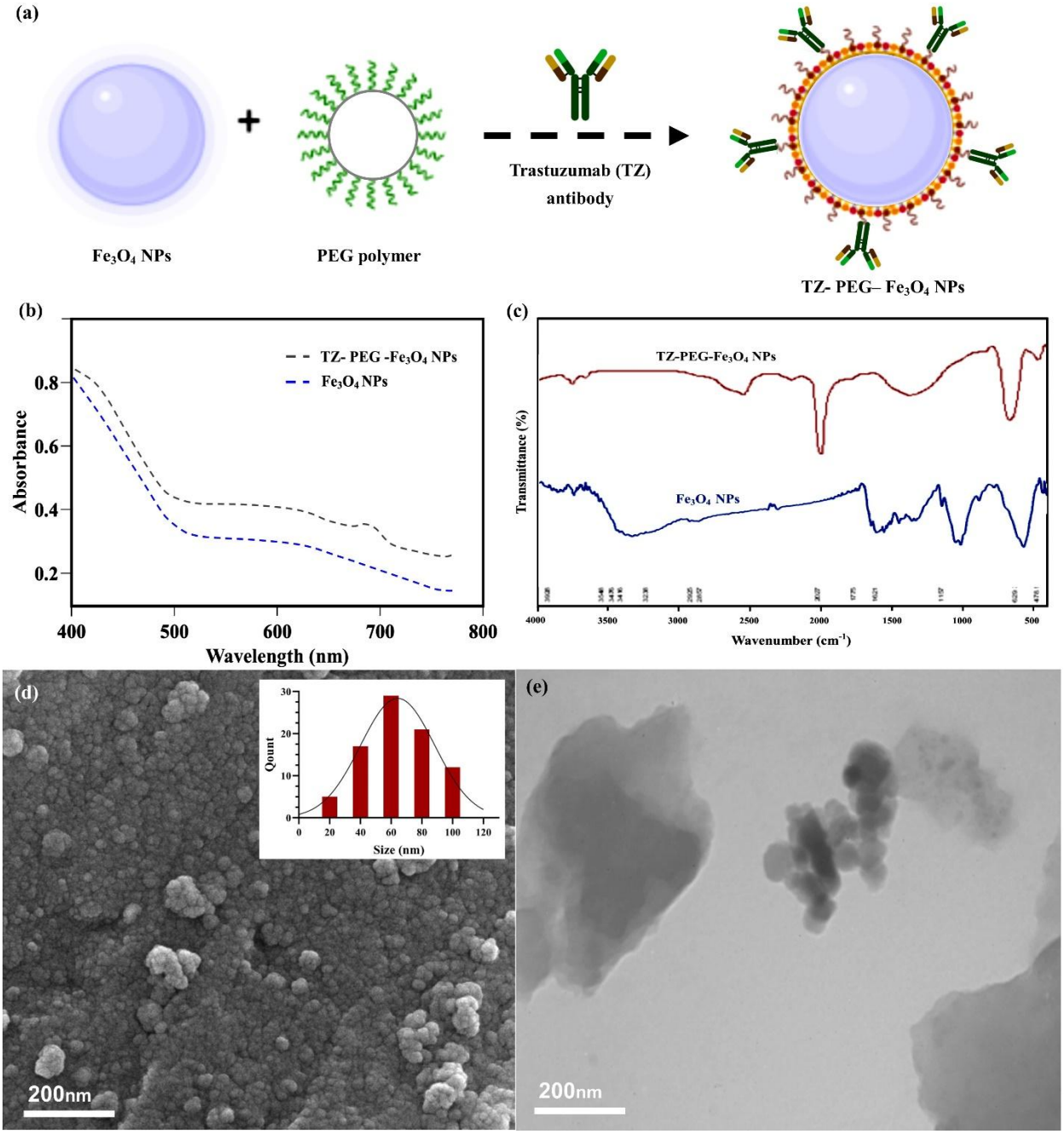


Figure 1. Characterization of TZ labeled PEGylated Fe_3O_4 nanoparticles (TZ-PEG-Fe_3O_4 NPs). **(a)** Schematic illustration showing the synthesis of TZ-PEG-Fe_3O_4 NPs, **(b)** Ultraviolet-visible (UV-vis) spectroscopy of the Fe_3O_4 NPs and TZ-PEG-Fe_3O_4 NPs, **(c)** Fourier transform infrared (FTIR) spectra of Fe_3O_4 NPs and TZ-PEG-Fe_3O_4 NPs, **(d)** Scanning electron microscopy (SEM) image of Fe_3O_4 NPs, and **(e)** Transmission electron microscopy (TEM) image of Fe_3O_4 NPs. Fe_3O_4 (iron oxide), PEG (polyethylene glycol), TZ (trastuzumab) and NPs (nanoparticles)

To validate the successful synthesis analyze the properties of the NPs, a range of comprehensive characterization techniques were employed. UV-vis (Figure 1b) and FTIR (Figure 1c) spectroscopy were utilized to investigate the optical properties of the advanced NPs and the molecular interactions and functional groups present on the surface of the NPs, revealing crucial information about their absorption and scattering characteristics in the visible range. The FTIR spectra exhibited characteristic peaks corresponding to the functional groups associated with both the Fe_3O_4 and TZ-PEG-Fe_3O_4 NPs, confirming successful functionalization.

Furthermore, TEM and SEM imaging techniques were employed to examine the morphology and size of the synthesized NPs in detail (Figure 1(d and e)). The imaging results confirmed a uniform spherical

structure with an average diameter of approximately 60 nm. This size is particularly advantageous for cellular uptake and interaction, making these NPs suitable candidates for drug delivery systems. Collectively, these characterization methods not only validated the successful synthesis of the Fe_3O_4 and TZ-PEG-Fe_3O_4 NPs but also provided valuable insights into their structural, optical, and functional properties.

3.2. Colloidal Stability Test

The colloidal stability of the synthesized NPs is a crucial factor for their effectiveness in biological uses. To assess the long-term stability of the TZ-PEG-Fe_3O_4 NPs in deionized PBS, we conducted a DLS analysis to measure changes in hydrodynamic size at room temperature (37°C) over a period of seven days. As illustrated in Figure 2a, the size of the TZ-PEG-Fe_3O_4 NPs in PBS remained relatively constant, indicating that the system maintained stability throughout the observation period. This stability can be attributed to a balanced interplay between attractive and repulsive forces within the environment. Additionally, the negative charge from the phosphate groups in PBS contributed to the colloidal stability of the NPs, which also possess negative surface charges (Figure 2a).

3.3. VSM Analysis Test

To evaluate the magnetic properties of the Fe_3O_4 and TZ-PEG-Fe_3O_4 NPs, the VSM was employed. The magnetic curves for bare Fe_3O_4 NPs and the composite TZ-PEG-Fe_3O_4 NPs were obtained at room temperature, as shown in Figure 2a. The analysis revealed that the saturation magnetization (Ms) of the uncoated Fe_3O_4 NPs was measured at 42 emu/g. However, after surface modification with PEG, the saturation magnetization value decreased to 34 emu/g. This reduction in magnetization can be attributed to the presence of the PEG chains, which may interfere with the magnetic interactions within the NPs. Furthermore, the absence of a residual loop in the magnetic curve indicates that the TZ-PEG-Fe_3O_4 NPs exhibit superparamagnetic behavior. Superparamagnetism is characterized by the lack of residual magnetization once the external magnetic field is removed, making these NPs particularly suitable for targeted drug delivery and MRI applications. The superparamagnetic nature of the TZ-PEG-Fe_3O_4 NPs suggests that they can be easily manipulated in a magnetic field, allowing for precise control over their movement and localization in biological systems. This property enhances their potential for being used in various biomedical applications, where controlled targeting and minimal toxicity are essential.

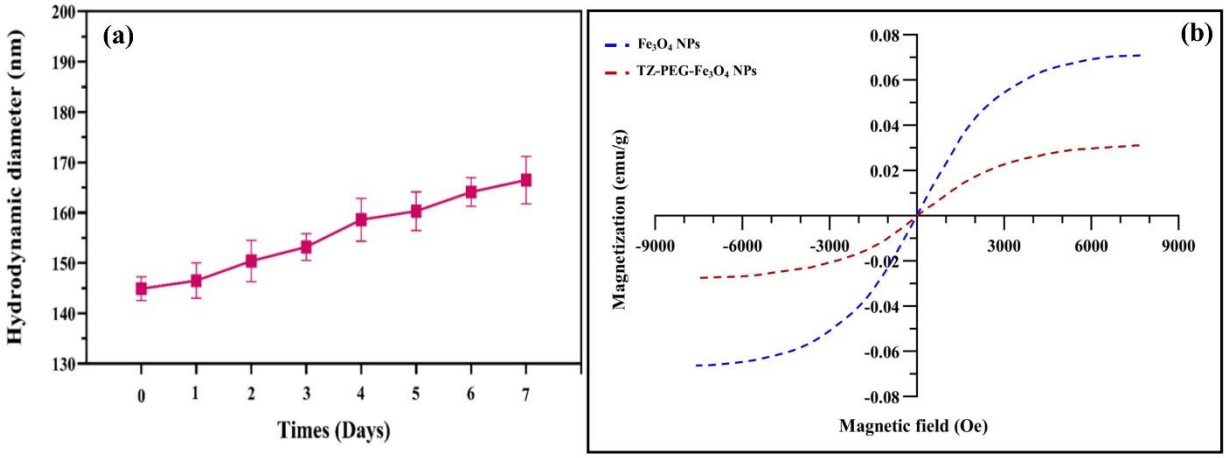


Figure 2. (a) The colloidal stability of TZ labeled PEGylated Fe_3O_4 nanoparticles (TZ-PEG-Fe_3O_4 NPs) by observing their hydrodynamic size using DLS examination over a period of 7 days in a simulated biological environment (PBS, pH=7.4), and (b) Magnetization versus applied magnetic field for Fe_3O_4 NPs and (b) TZ-PEG-Fe_3O_4 NPs. Fe_3O_4 (iron oxide), PEG (polyethylene glycol), TZ (trastuzumab), and NPs (nanoparticles)

3.4. Cytotoxicity of TZ-PEG-Fe_3O_4 NPs

The cell viability study was conducted to assess the cytotoxic effects of the advanced targeted TZ-PEG-Fe_3O_4 NPs on both MCF-10A normal breast cells and SKBr-3 BC cells. The cells were exposed to variable concentrations of NPs for durations of 24 and 48 hours, with the results illustrated in Figure 3(a & b).

The findings indicated that both cell lines, MCF-10A and SKBr-3, exhibited high cell viability, even at NPs concentrations up to 100 µg/ml. In the case of the MCF-10A healthy cell line, minimal cell damage was observed after 24 and 48 hours of exposure to the NPs. Conversely, the SKBr-3 cancer cell line showed a greater degree of cell damage over the same periods, particularly at the 48-hour mark and at higher concentrations. These results suggest that the TZ-PEG-Fe_3O_4 NPs do not exert significant cytotoxic effects on either cell type within the tested concentration range and exposure times, indicating their potential safety in therapeutic applications.

3.5. In-Vitro MR Imaging

To evaluate the targeting capabilities of the synthesized TZ-PEG-Fe_3O_4 NPs, SKBr-3 BC cells, and MCF-10A normal breast cells were treated with different concentrations (0, 1, and 10 µg/mL) of TZ-PEG-Fe_3O_4 NPs, alongside a control group receiving

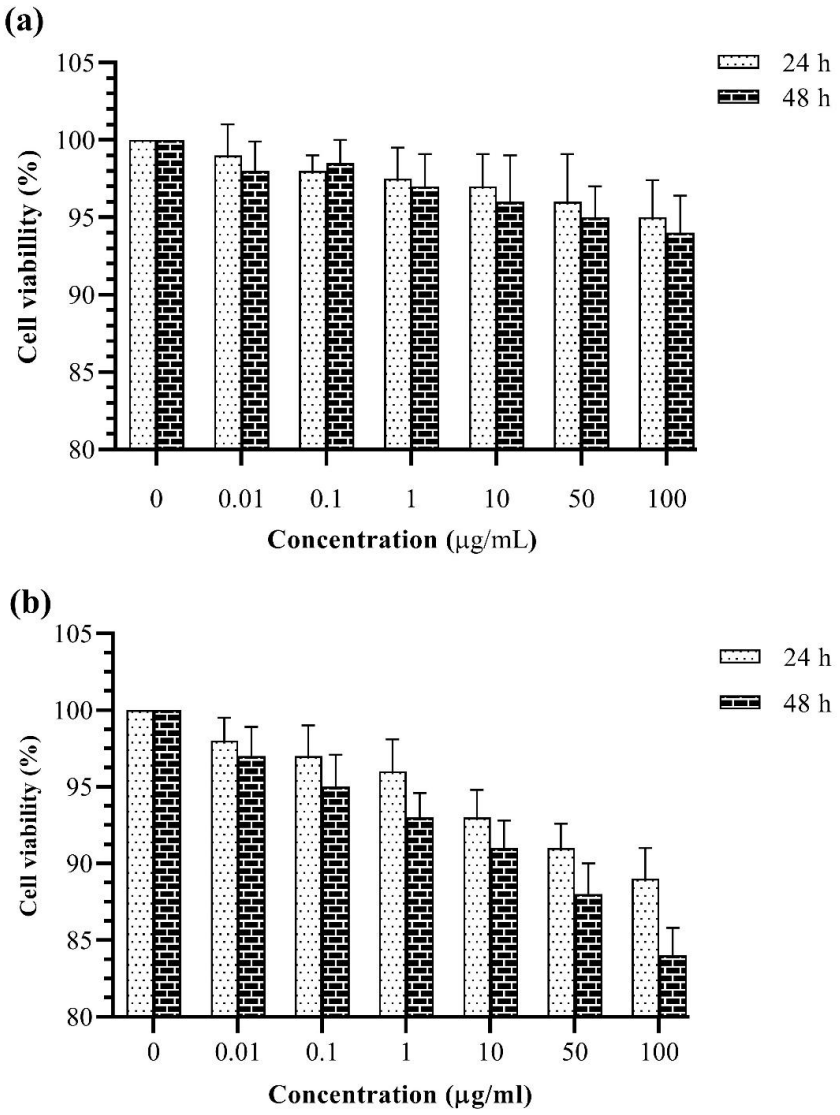


Figure 3. Cytotoxicity of TZ labeled PEGylated Fe_3O_4 nanoparticles (TZ-PEG-Fe_3O_4 NPs) measured by MTT assay in MCF 10A (a) and SKBr-3 (b) after 24 and 48 h incubation. Fe_3O_4 (iron oxide), PEG (polyethylene glycol), TZ (trastuzumab), and NPs (nanoparticles)

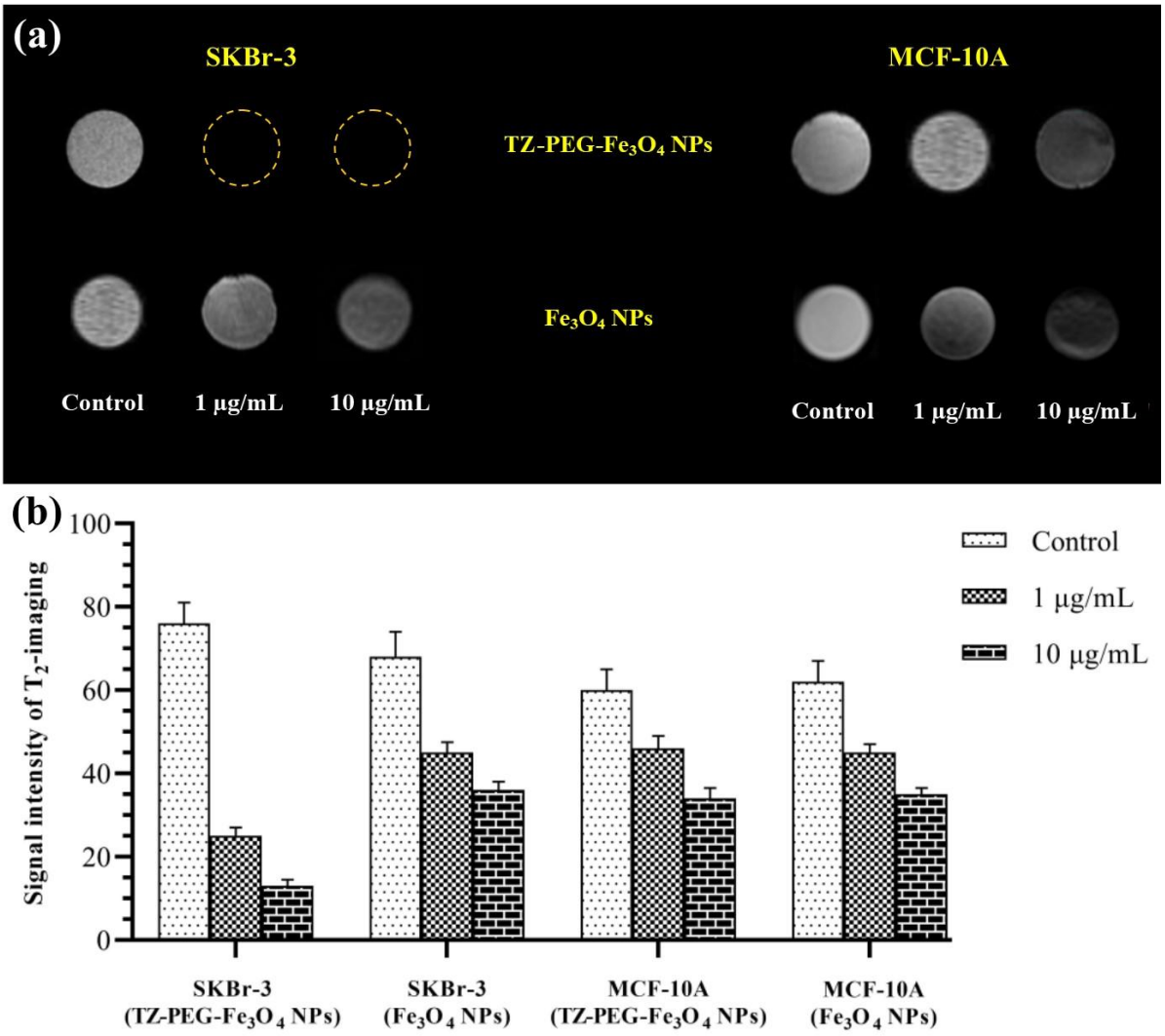


Figure 4. T_2-weighted MR images of TZ-PEG-Fe_3O_4 NPs in MCF-10A and SKBr-3 cells at different concentrations following incubation for 6 h produced by a 1.5 T MR system (a), and signal intensity analysis for T_2-weighted MR images (b). Fe_3O_4 (iron oxide), PEG (polyethylene glycol), TZ (trastuzumab), and NPs (nanoparticles)

only Fe_3O_4 NPs. Each cell type was plated at a density of 4×10^5 cells per well and incubated for 6 hours at room temperature. After incubation, the cells were washed three times with PBS to eliminate any unbound NPs. The cells were then resuspended in PBS at a concentration of 1×10^5 cells/mL, preparing them for MRI. All MR imaging was performed using a 1.5 Tesla MRI system. T2-weighted MR imaging utilized a fast spin-echo sequence optimized for minimal acquisition time. The imaging parameters included a Repetition Time (TR) of 3600 ms, an Echo Time (TE) of 90 ms, a matrix size of 220 × 320, a FOV of 82 × 120 mm², a bandwidth of 220 Hz/Px, and a slice thickness of 2 mm. The findings from this test shed light on the effectiveness of TZ-PEG-Fe_3O_4 NPs in targeting specific cell types, especially in differentiating between normal and cancerous cells.

4. Discussion

In the present study, the use of targeted superparamagnetic TZ-PEG-Fe_3O_4 NPs as CAs in T2-weighted MRI was investigated. The TEM and SEM images revealed that the synthesized TZ-PEG-Fe_3O_4 NPs had a roughly spherical shape, with well-separated individual particles and some small aggregates. A schematic diagram in Figure 1a illustrates the structure of the Fe_3O_4 NPs coated with a PEG layer and labeled with TZ. Analysis of the TEM data showed that the final NPs had a relatively uniform size distribution. The images demonstrated a consistent shape and size across the sample, with an average diameter of approximately 60 nm. The size distribution of the NPs fell within the desired range. The small size of the NPs, below 100 nm,

offers several potential advantages for their applications. NPs smaller than 100 nm tend to exhibit high colloidal stability, which is crucial for maintaining their integrity and functionality during storage and administration. The small size of the NPs also offers several advantages, including the ability to exploit the EPR effect. The EPR effect is a phenomenon observed in tumor tissues, where leaky blood vessels and impaired lymphatic drainage allow for the accumulation of NPs within the tumor microenvironment. Due to their small size, the TZ-PEG-Fe_3O_4 NPs can easily penetrate the leaky blood vessel walls surrounding the tumor and accumulate in the tumor tissue. This passive targeting strategy takes advantage of the EPR effect, allowing for selective accumulation of the NPs in the tumor while minimizing accumulation in healthy tissues [20]. Leveraging the EPR effect, the TZ-PEG-Fe_3O_4 NPs have the potential to specifically accumulate in tumor tissues, enhancing their effectiveness as a targeted imaging agent. Furthermore, the NPs' small size facilitates their delivery to tumor sites, as they can easily traverse the tumor vasculature and reach the target cells. The findings of this study align with previous research in several key aspects. For instance, Dousset *et al.* conducted a comparative analysis of USPIO-enhanced MRI against conventional T2-weighted MRI and gadolinium-enhanced T1-weighted MRI in a model of Experimental Autoimmune Encephalomyelitis (EAE). Their results demonstrated that USPIO-enhanced MRI exhibited high sensitivity for detecting EAE lesions, successfully identifying lesions in 8 out of 9 animals, while conventional T2-weighted MRI and gadolinium-enhanced T1-weighted MRI showed significantly lower sensitivities, detecting lesions in only 1 out of 9 and 0 out of 9 animals, respectively. These results suggest that USPIO-enhanced MRI may serve as a more effective tool for detecting macrophage-related pathologies, such as those associated with EAE, compared to traditional MRI methods. The improved sensitivity of USPIO-enhanced MRI could be particularly beneficial for early disease detection and ongoing monitoring [21].

The results from the FTIR spectroscopy and magnetization studies provide significant insights into the structural and functional characteristics of the synthesized Fe_3O_4 NPs and TZ-PEG-Fe_3O_4 NPs, particularly in the context of their potential applications in targeted MRI. The FTIR spectroscopy results indicated the successful functionalization of the Fe_3O_4 NPs and TZ-PEG-Fe_3O_4 NPs with hydroxyl (–OH) groups and the TZ antibody [22]. The presence of characteristic peaks corresponding to H-O bending and stretching vibrations suggests that the NPs maintain a hydrophilic surface, which is essential for enhancing their colloidal stability in biological environments. The detection of peaks associated with anti-HER-2 further confirms that the NPs have been effectively conjugated with the antibody, which is crucial for targeting specific cancer cells, such as those overexpressing the HER-2 receptor [19]. The amide stretching vibrations observed at 3430.9 cm^{-1} and 1630.21 cm^{-1} indicate that the conjugation process is not only successful but also retains the functional integrity of the TZ antibody. This is particularly important because the biological activity of the antibody must be preserved to ensure effective targeting and therapeutic efficacy. The alignment of these findings with previous studies reinforces the reliability of the synthesis and functionalization methods employed. Furthermore, the magnetization analysis reveals that the Ms of the uncoated Fe_3O_4 NPs is 42 emu/g, which decreases to 34 emu/g after the addition of the PEG coating and the TZ antibody. This reduction in magnetization can be attributed to the presence of the non-magnetic PEG layer and the antibody, which may hinder magnetic interactions among the NPs [5]. Despite this decrease, the superparamagnetic behavior exhibited by the TZ-PEG-Fe_3O_4 NPs is advantageous for biomedical applications. The absence of a hysteresis loop indicates that the NPs will not retain magnetization once an external magnetic field is removed, minimizing the risk of aggregation and enhancing their circulation time in the bloodstream. The combination of superparamagnetic properties and the ability to target specific cell types positions the TZ-PEG-Fe_3O_4 NPs, as promising candidates in targeted imaging. The EPR effect, which allows for the preferential accumulation of NPs in tumor tissues, can be further exploited due to the NPs small size and surface functionalization. This targeted approach not only increases the effectiveness of imaging but also enhances the potential for therapeutic applications, allowing for the delivery of CAs directly to cancer cells while minimizing exposure to healthy tissues [23].

The in-vitro results depicted in Figure 3a and 3b provide compelling evidence for the biocompatibility of the TZ-PEG-Fe_3O_4 NPs across a concentration range of 0-100 µg/mL. These findings suggest that the NPs can be utilized in biological applications without causing significant harm to cells. The MTT assay demonstrated

a notable decrease in cell viability with increased exposure time to the TZ-PEG-Fe_3O_4 NPs, particularly in SKBr-3 BC cells. In contrast, the cytotoxic effects on MCF-10A non-tumorigenic cells were significantly lower across all tested concentrations (P-value < 0.05).

The differential cytotoxicity observed between the SKBr-3 and MCF-10A cell lines can be attributed to the varying expression levels of the TZ receptor, HER-2. SKBr-3 cells, which overexpress HER-2, exhibited heightened sensitivity to the cytotoxic effects of the NPs. This increased susceptibility is likely due to the enhanced binding affinity of the TZ-PEG-Fe_3O_4 NPs to the HER-2 receptors, facilitating their internalization and subsequent cytotoxic effects. Importantly, the TZ-PEG-Fe_3O_4 NPs demonstrated minimal cytotoxicity toward MCF-10A cells, even at higher concentrations, indicating their potential biocompatibility and safety for use in therapeutic applications.

These findings underscore the potential of TZ-PEG-Fe_3O_4 NPs as targeted CAs in biomedical applications, particularly for imaging and treating SKBr-3 BC cells that exhibit higher HER-2 expression. The results align with previous studies that have explored the cytotoxic effects of TZ-conjugated NPs on cancer cells. For example, research by Cai *et al.* investigated the effects of TZ-conjugated gold (TZ-Au) NPs on SKBr-3 cells, revealing that these NPs demonstrated a significant binding affinity and were efficiently internalized compared to unconjugated Au NPs. This increased internalization resulted in enhanced DNA damage, evidenced by a rise in double-strand breaks, and a reported 55% decrease in cell viability upon exposure to TZ-Au NPs.

The implications of these findings are substantial, as they suggest that the TZ-PEG-Fe_3O_4 NPs could be developed into effective imaging agents that selectively target HER-2 positive BC cells while sparing normal cells. This selective targeting not only enhances the diagnostic value but also minimizes potential side effects associated with conventional treatments such as radiotherapy.

The cell viability of SKBr-3 cells treated with TZ-PEG-Fe_3O_4 NPs was measured at 92.6% and 88.7% after 24 and 48 hours of treatment, respectively. In comparison, MCF-10A cells exhibited slightly higher viability rates of 97.4% and 94.5% after the same treatment durations, with a nanoparticle concentration of 100 µg/mL. This difference in cell viability can be attributed to the overexpression of the HER-2 receptor on the surface of SKBr-3 cells, which facilitates the selective accumulation of the NPs in cancerous cells through active targeting mechanisms. Also, relaxivity measurements indicated that the TZ-PEG-Fe_3O_4 NPs maintained appropriate relaxivity values even after being coated with PEG, a hydrophilic polymer. This phenomenon may be due to the presence of polar carbonyl groups on the surface of the Fe_3O_4, as noted in previous studies, including those by Fang *et al.* It is important to note that the r2 values are influenced by factors such as the type of NPs, hydrodynamic diameter, and the properties of the ligands or coating agents surrounding the magnetic ions. The favorable T2 value of the TZ-PEG-Fe_3O_4 NPs can be attributed to the susceptibility of the superparamagnetic Fe_3O_4 component.

The in-vitro MRI results demonstrated a significant contrast difference in MR images between MCF-10A and SKBr-3 cells, which can be linked to the specific uptake of TZ-PEG-Fe_3O_4 NPs by SKBr-3 cells due to HER-2 receptor overexpression. This experiment clearly indicates that the specific binding and uptake of the NPs are mediated by the interaction between TZ and the HER-2 receptor on the cell surface. The findings suggest that TZ-PEG-Fe_3O_4 NPs can effectively influence T2MR signals through HER-2-mediated cell binding and uptake. The targeted T2-weighted MRI assessments confirmed the specific and enhanced intracellular accumulation of TZ-PEG-Fe_3O_4 NPs in SKBr-3 cancer cells, highlighting the significant role of the TZ-induced targeting moiety. Similar findings were reported by Kim *et al.*, who noted that surface modifications of Fe_3O_4 NPs can significantly alter transverse relaxivity, achieving r_2 values of 245 $mM^{-1}s^{-1}$ at 1.5 T and 211.8 $mM^{-1}s^{-1}$ at 3 T [24]. These enhanced relaxivity values underscore the potential of these NPd as effective T2 CAs in MRI applications. Therefore, the results of this study demonstrate the promising capabilities of TZ-PEG-Fe_3O_4 NPs in targeted imaging applications, particularly for HER-2 positive BC cells. This targeted approach not only improves imaging contrast but also paves the way for future therapeutic applications, where such NPs could be employed in combined diagnostic and treatment strategies, enhancing the overall efficacy of cancer management. Also, the synthesis and characterization of Fe/Fe_3O_4 nanocubes, as reported by Waleed E. Mahmoud *et al.*, align with the findings of the current

study in several aspects. They revealed that the Fe/Fe_3O_4 nanocubes exhibited superparamagnetic behavior at room temperature, with a saturation magnetization of 129 emu/g. This finding is consistent with the superparamagnetic properties observed in the TZ-PEG-Fe_3O_4 NPs synthesized in the current study, as evidenced by the absence of a hysteresis loop in the magnetization curve. The high saturation magnetization value reported by Mahmoud *et al.* suggests that the Fe/ Fe_3O_4 could serve as effective CAs for MRI, similar to the potential applications of the TZ-PEG-Fe_3O_4 NPs in the current study [25].

Similarly, Sousa *et al.* explored the application of nanoparticle-based MRI T2negative CAs by synthesizing two classes of mixed-ligand protected bimetallic iron NPs (Fe NPs). Their cellular studies indicated that these Fe NPs exhibited minimal toxicity, making them suitable for biomedical applications. MRI phantom experiments demonstrated that the r_2/r_1 ratio of the Fe NPs reached an impressive 670, resulting in a 66% reduction in T2 relaxation time. These findings suggest that the synthesized Fe NPs have significant potential as diagnostic and therapeutic imaging CAs. The high r_2/r_1 ratio indicates that the Fe NPs can effectively enhance MRI contrast, which is particularly valuable in clinical settings where precise imaging is crucial for diagnosis and treatment planning. As well as the current study, the limited toxicity observed in cellular studies further supports the feasibility of using these NPs in-vivo, as they are less likely to cause adverse effects in patients [26].

The research conducted by Parvaneh *et al.* aligns with the current study in several key aspects, particularly in exploring the potential of magnetic-based detection techniques to enhance the sensitivity and quantification of Hepatitis B Virus (HBV) infection. In their study, they initially modified Fe_3O_4 NPs using silica and chitosan, followed by labeling the anti-HBsAg antibodies onto these modified magnetic NPs. Their findings demonstrated the effectiveness of the developed antibody-conjugated magnetic NPs for sensitive detection of HBsAg, with binding capacity comparable to commercially available products. This conjugation strategy offers a promising approach for producing high-capacity magnetic NPs suitable for a range of biomedical applications, including the detection and quantification of HBV infection [27].

As mentioned, MRI has been a widely used diagnostic tool in medicine, often enhanced by CAs to improve image quality. The most commonly utilized CAs are gadolinium-based CAs, but their use has raised concerns regarding potential metal accumulation in essential organs. To address these issues, researchers led by Marasini *et al.* explored alternative CAs, specifically paramagnetic iron (III) ionic chelate NPs. The NPs also showed strong relaxivity properties, suggesting their potential for use in contrast-enhanced MRI. Notably, the relaxivity of these NPs was approximately three times greater than that of the clinical Magnevist®, highlighting their potential for improved imaging in various medical conditions. This enhanced performance indicates that paramagnetic iron-based NPs could be effective alternatives to traditional gadolinium-based agents, reducing the risks associated with metal accumulation while providing superior imaging capabilities [28].

5. Conclusion

In this study, we explored the potential of modified Fe_3O_4 NPs as targeted Contrast Agents (CAs) for MR imaging in breast tumor diagnosis. Our findings confirmed the biocompatibility of Fe_3O_4 NPs, as evidenced by the sustained viability of SKBr-3 BC cells even at varying NPs concentrations. The TZ-PEG-Fe_3O_4 NPs demonstrated significant promise for enhancing MRI capabilities and improving diagnostic accuracy across a range of medical applications. The ability of these NPs to selectively target tumor cells while remaining non-toxic to healthy cells highlights their potential for clinical use. The targeted nature of the TZ-PEG-Fe_3O_4 NPs, combined with their favorable magnetic properties, positions them as effective agents for contrast-enhanced MRI, which is crucial for accurate tumor detection and characterization.

Furthermore, the results of this study suggest that the incorporation of targeting ligands, such as trastuzumab, can enhance the specificity of imaging agents, leading to improved visualization of tumors. This approach not only aids in the early detection of cancer but also has implications for monitoring treatment responses and disease progression. Given the promising results, further research and optimization are necessary to fully harness the potential of targeted Fe_3O_4 NPs in clinical settings.

References

1- Ghorbani M Ayyami Y, Dastgir M, Malekzadeh R, Mortezazadeh T. Chitosan-modified manganese oxide-conjugated methotrexate nanoparticles delivering 5-aminolevulinic acid as a dual-modal T1–T2* MRI contrast agent in U87MG cell detection. Magnetic Resonance Materials in Physics, Biology and Medicine. 2024 May 25:1-6.

2- Tarighatnia A Mohaghegh S, Omidi Y, Barar J, Aghanejad A, Adibkia K. Multifunctional magnetic nanoparticles for MRI-guided co-delivery of erlotinib and L-asparaginase to ovarian cancer. Journal of Microencapsulation. 2022 May 19;39(4):394-408.

3- Tarighatnia A Jamshidi N, Ghaziyani MF, Sajadian F, Olad-Ghaffari M, Nader ND. Folic acid-conjugated Fe-Au-based nanoparticles for dual detection of breast cancer cells by magnetic resonance imaging and computed tomography. Frontiers in Biomedical Technologies. 2023 Dec 26.

4- Khoei S Amraee A, Mahdavi SR, Tohidkia MR, Tarighatnia A, Darvish L, Hosseini Teshnizi S, Aghanejad A. Ultrasmall iron oxide nanoparticles and gadolinium-based contrast agents in magnetic resonance imaging: a systematic review and meta-analysis. Clinical and Translational Imaging. 2023 Feb;11(1):83-93.

5- Babaye Abdollahi B Malekzadeh R, Ghorbani M, Pirayesh Islamian J, Mortezazadeh T. Trastuzumab conjugated PEG–Fe3O4@ Au nanoparticle as an MRI biocompatible nano-contrast agent. International Journal of Polymeric Materials and Polymeric Biomaterials. 2023 Jul 3;72(10):759-70.

6- Ghorbani M Malekzadeh R, Faghani P, Abdollahi BB, Mortezazadeh T, Farhood B. Fabrication of targeted gold nanoparticle as potential contrast agent in molecular CT imaging. Journal of Radiation Research and Applied Sciences. 2023 Mar 1;16(1):100490.

7- Malekzadeh R Ziyaee S, Ghorbani M, Nasiri Motlagh B, Asghariazar V, Mortezazadeh T. Preparation of MnO2@ poly-(DMAEMA-co-IA)-conjugated methotrexate nano-complex for MRI and radiotherapy of breast cancer application. Magnetic Resonance Materials in Physics, Biology and Medicine. 2023 Oct;36(5):779-95.

8- Ayyami Y Yektamanesh M, Ghorbani M, Dastgir M, Malekzadeh R, Mortezazadeh T. Characterization of multifunctional β-cyclodextrin-coated Bi2O3 nanoparticles conjugated with curcumin for CT imaging-guided synergetic chemo-radiotherapy in breast cancer. International Journal of Pharmaceutics. 2024 Jun 25;659:124264.

9- Mortezazadeh T Alipour B, Abdulsahib WK, Arzhang A, Malekzadeh R, Farhood B. A systematic review of multimodal application of quantum dots in breast cancer diagnosis: Effective parameters, status and future perspectives. Journal of Drug Delivery Science and Technology. 2023 Sep 1;86:104682.

10- Xuan S J Wang YX, Port M, Idee JM. Recent advances in superparamagnetic iron oxide nanoparticles for cellular imaging and targeted therapy research. Current pharmaceutical design. 2013 Nov 1;19(37):6575-93.

11- Park J Yu MK, Jon S. Targeting strategies for multifunctional nanoparticles in cancer imaging and therapy. Theranostics. 2012;2(1):3.

12- Vega MA Nieto C, Martin del Valle EM. Trastuzumab: more than a guide in HER2-positive cancer nanomedicine. Nanomaterials. 2020 Aug 26;10(9):1674.

13- Araujo F Nunes R, Tavares J, Sarmento B, das Neves J. Surface modification with polyethylene glycol enhances colorectal distribution and retention of nanoparticles. European Journal of Pharmaceutics and Biopharmaceutics. 2018 Sep 1;130:200-6.

14- Development and Applications of the Silica-Based Contrast Agents in Magnetic Resonance Imaging. Current Nanomedicine (Formerly: Recent Patents on Nanomedicine). 2018 Apr 1;8(1):3-27. Chowdhury MA. Design.

15- Gao L Yang M, Liu K, Luo C, Wang Y, Yu L, Peng H, Zhang W. Characterization of Fe3O4/SiO2/Gd2O (CO3) 2 core/shell/shell nanoparticles as T1 and T2 dual mode MRI contrast agent. Talanta. 2015 Jan 1;131:661-5.

16- Gholibegloo E Mansouri H, Mortezazadeh T, Yazdi MH, Ashouri F, Malekzadeh R, Najafi A, Foroumadi A, Khoobi M. A biocompatible theranostic nanoplatform based on magnetic gadolinium-chelated polycyclodextrin: in vitro and in vivo studies. Carbohydrate Polymers. 2021 Feb 15;254:117262.

17- Phinikaridou A Sandiford L, Protti A, Meszaros LK, Cui X, Yan Y, Frodsham G, Williamson PA, Gaddum N, Botnar RM, Blower PJ. Bisphosphonate-anchored PEGylation and radiolabeling of superparamagnetic iron oxide: long-circulating nanoparticles for in vivo multimodal (T1 MRI-SPECT) imaging. Acs Nano. 2013 Jan 22;7(1):500-12.

18- Han B Wei Y, Hu X, Lin Y, Wang X, Deng X. Synthesis of Fe3O4 nanoparticles and their magnetic properties. Procedia Engineering. 2012 Jan 1;27:632-7.

19- Ghorbani M Abdollahi BB, Hamishehkar H, Malekzadeh R, Farajollahi A. Synthesis and characterization of actively HER-2 Targeted Fe3O4@ Au nanoparticles for molecular radiosensitization of breast cancer. BioImpacts: BI. 2023;13(1):17.

20- Yang K Zi Y, He J, Wu Z, Liu J, Zhang W. Strategies to enhance drug delivery to solid tumors by harnessing the EPR effects and alternative targeting mechanisms. Advanced Drug Delivery Reviews. 2022 Sep 1;188:114449.

21- Ballarino L Dousset V, Delalande C, Coussemacq M, Canioni P, Petry KG, Caillé JM. Comparison of ultrasmall particles of iron oxide (USPIO)-enhanced T2-weighted, conventional T2-weighted, and gadolinium-enhanced T1-weighted MR images in rats with experimental autoimmune encephalomyelitis. American journal of neuroradiology. 1999 Feb 1;20(2):223-7.

22- Singh LH Pati SS, Guimarães EM, Mantilla J, Coaquira JA, Oliveira AC, Sharma VK, Garg VK. Magnetic chitosan-functionalized Fe3O4@ Au nanoparticles: Synthesis and characterization. Journal of Alloys and Compounds. 2016 Nov 5;684:68-74.

23- Wang K Gao Y, Zhang J, Duan X, Sun Q, Men K. Multifunctional nanoparticle for cancer therapy. MedComm. 2023 Feb;4(1):e187.

24- Kim HS Kim J, Lee N, Kim T, Kim H, Yu T, Song IC, Moon WK, Hyeon T. Multifunctional uniform nanoparticles composed of a magnetite nanocrystal core and a mesoporous silica shell for magnetic resonance and fluorescence imaging and for drug delivery. Angewandte Chemie-International Edition. 2008 Oct 20;47(44):8438-41.

25- Bronstein LM Mahmoud WE, Al-Hazmi F, Al-Noaiser F, Al-Ghamdi AA. Development of Fe/Fe3O4 core–shell nanocubes as a promising magnetic resonance imaging contrast agent. Langmuir. 2013 Oct 22;29(42):13095-101.

26- Sanavio B Sousa F, Saccani A, Tang Y, Zucca I, Carney TM, Mastropietro A, Jacob Silva PH, Carney RP, Schenk K, Omrani AO. Superparamagnetic nanoparticles as high efficiency magnetic resonance imaging T2 contrast agent. Bioconjugate chemistry. 2017 Jan 18;28(1):161-70. .

27- Khademi F Parvaneh S, Abdi G, Alizadeh A, Mostafaie A. Efficient conjugation of anti-HBsAg antibody to modified core-shell magnetic nanoparticles (Fe3O4@ SiO2/NH2). BioImpacts: BI. 2021;11(4):237.

28- Rayamajhi S Marasini R, Moreno-Sanchez A, Aryal S. Iron (iii) chelated paramagnetic polymeric nanoparticle formulation as a next-generation T 1-weighted MRI contrast agent. RSC advances. 2021;11(51):32216-26.